International Journal of Innovative Computing, Information and Control
Volume **9**, Number **9**, September **2013**

ICIC International ©2013 ISSN 1349-4198
pp. 3759–3777

SUPPRESSION OF HAND TREMOR MODEL USING ACTIVE FORCE CONTROL WITH PARTICLE SWARM OPTIMIZATION AND DIFFERENTIAL EVOLUTION

Azizan As'arry, Mohd Zarhamdy Md. Zain, Musa Mailah and Mohamed Hussein

Department of System Dynamics and Control
Faculty of Mechanical Engineering
Universiti Teknologi Malaysia
81310 UTM Johor Bahru, Johor, Malaysia
wertzizan@yahoo.com; {zarhamdy; musa; mohamed}@fkm.utm.my

Received July 2012; revised December 2012

Abstract. *Debilitating conditions for patients with hand tremor may find their daily activities such as writing and holding objects affected. In order to provide a non-invasive solution, an active tremor control technique is proposed to suppress a human hand tremor model. In this study, a hybrid controller which is a combination of the classic Proportional-Integration-Derivative (PID) and Active Force Control (AFC) strategy is employed to a four degree-of-freedom (4-DOF) biodynamic model of a human hand. In this study, two intelligent optimization techniques, namely, the Particle Swarm Optimization (PSO) and Differential Evolution (DE) methods are employed to estimate the PID and AFC parameters. The findings of the study demonstrate that the hybrid controller gives excellent performance in reducing the tremor error in comparison with the classic pure PID controller. Based on the fitness evaluation, the AFC-based scheme enhances the PID controller performance by about 25% for both PSO and DE techniques. The numerical simulation work could be used as an initial stage of study for the development of an anti tremor device for use on actual human subject that utilizes linear voice coil actuator as the main active suppressive element.*

Keywords: Hybrid active tremor control, Particle swarm optimization, Differential evolution, Linear voice coil actuator

1. **Introduction.** Tremor is an involuntary muscle movement that can affect the hand and head. Tremor can be embarrassing and make it harder to perform daily tasks. It features like a "pill-rolling"; thumb and index finger keep on rubbing and perform a circular movement. Tremor may happen to everyone and most Parkinson disease (PD) patients are not concerned at the early stage of their tremor until the tremor becomes worse [1]. Tremor originates from damaged brain cells that affect the human nerve muscle. It occurs due to the degeneration of dopaminergic neurons in the Substantia Nigra (located in the upper portion of the midbrain) [2]. Dopamine is a vital chemical transmitter in the brain. The shortage of dopamine (less than 80% of dopamine in the brain) reduces transmission and this poses a problem to the nerve cells connected to each other to control muscle or motor behavior [3] consequently causing tremor. Perhaps patients may do several tasks; however, the debilitating condition may limit their efforts to perfectly perform the desired tasks especially in holding and writing. In addition, they also face other problems like depression, sleep problem or speaking.

In order to abate tremor, PD patients are normally treated with drugs, physiology therapy or surgical technique. These treatments can lessen the progression of tremor, but

do not heal the tremor [4]. Long term consumption of drugs may give negative side effects [5] and surgical technology seems like the best option, but the treatment is very costly and risky [4]. Among the estimated 15,000 Parkinson disease patients in Malaysia, about 1000 of them require high risk surgery, namely Deep Brain Stimulation (DBS) surgery to survive [6]. In public hospitals, the cost is RM 80,000 for the first surgery and RM 60,000 for battery replacement every 3-5 years [6].

A lot of efforts and researches have surfaced on the use of biomechanical means as the alternative approach for tremor suppression. The idea is to practice an engineering method by developing an external device either to wear or in contact with the human body part to be controlled. This non-invasive method mainly targets the human hand by sensing the tremor behavior and cancelling it using a smart actuator system. The active tremor control is not intended to continuously lessen human hand tremor but applied when necessary to assist a patient in performing specific tasks for a certain period of time. Some successful simulation and experimental results have been reported, such as using DC motor [7], functional electrical stimulation [8] and magnetorheological (MRF) [9].

Motivated by a desire to develop active tremor control, the work is intended to formulate a numerical study of hybrid Proportional, Integral and Derivative (PID) and Active Force Control (AFC) control schemes. An intelligent mechanism, based on Particle Swarm Optimization (PSO) and Differential Evolution (DE) is employed to optimize the controller parameters. These optimizations are selected due to their capabilities in achieving high efficiency in searching for global optimal solution. Both techniques are able to compute fitness function and minimize tremor error but they have different strategies and computational effort.

The PSO algorithm was first introduced by Eberhart and Kennedy in the mid 1995s [10]. The numbers of published papers related to PSO are mainly related to optimal solution problem in control applications, especially in the tuning of PID parameters [11,12]. The algorithm is also able to solve for complex process, nonlinear constrain and multi-objective problems [13]. Meanwhile, the DE was first proposed by Price and Storn in 1995 where they discovered the procedure of using differential mutation combined with discrete recombination and pairwise selection without annealing factors [14]. Since then, the algorithm has become familiar and regularly practiced especially during the last decade [15,16]. DE demonstrates excellent performance in determining global optimal solution with lesser parameters to be tuned. Some advantages of DE are its simple structure, ease of use, rapid convergence and robustness [17].

Previous researches about the Active Force Control (AFC) have demonstrated the effectiveness of the AFC scheme applied to rigid robot arms [18-20]. To enhance the capability of AFC, Mailah et al. introduced the intelligent AFC scheme based on genetic algorithm to control a rigid two-link horizontal planar robotic arm [21]. Other Artificial Intelligent (AI) techniques such as neural network, fuzzy logic and iterative learning techniques have also been implemented in AFC-based schemes to estimate the controller parameters [22-24]. Inspired by the success of AFC strategy in vibration control, thus the subject of tremor control would be another interesting application. To the best of the authors' knowledge, the present study is a novel DE and PSO-based approach to optimally design the PID and AFC controller utilizing a linear voice coil actuator. The Biodynamic Response (BR) with Four Degree-of-Freedom (4-DOF) model will be used to generate the tremor motion and the mechanism to control tremor was developed in order to facilitate the control systems modeling and tuning. The numerical simulation work could be used

as an initial stage of study for the development of an anti tremor device for use on actual human subject that utilizes linear voice coil actuator as the main active suppressive element.

The paper is organized as follows. In Section 2, the plant model based on the 4-DOFs biodynamic response of the human hand is discussed. In Section 3, the dynamic modeling of the electromagnet actuator is formulated. In Section 4, the PID and AFC control theories are described. In Section 5, the optimal solutions for GA and DE techniques are presented. Results and discussion are presented in Section 6 and finally the conclusions are presented in Section 7.

2. **Biodynamic Model of the Human Hand.** The biodynamic response (BR) of the human hand is used to observe the relationship between the force and motion of human tremor. In this study, a mechanical model of a human hand is set up. The model represents a 4-DOF mass-spring-damper system to observe vibration transmissibility.

The idea of the BR study is to quantify the nature of the vibrations transmitted to different segments of the human palm in the vertical plane (z-axis) in terms of the amplitude behavior [25], as shown in Figure 1. In the simulation work, the dynamics of the system represents the relationship between the forces, acceleration and displacement in the hand. The acceleration signal will be multiplied by the estimated mass, the value of which is then used as an estimated disturbance and fed into the AFC feed forward loop. Meanwhile, the displacement signal will be used as a feedback closed loop signal to reduce the error of tremor.

In the 4-DOF model, the masses m_1, m_2, m_3 and m_4 are attributed to masses due to epidermis, dermis, subcutaneous tissue and the muscle, respectively. The coupling elements k_1 and c_1 represent the visco-elastic properties of the epidermis and dermis tissue. The strong coupling between the dermis and the subcutaneous tissue are related to k_2 and c_2. k_3 and c_3 represent the weak coupling between the subcutaneous tissue and the muscle. The elements k_4 and c_4 relate to the coupling between the muscle and bones [26].

The second order mass-spring-damper system can be readily simulated using MATLAB and Simulink software. The basic equation of motion of the 4-DOF model at the palm of human hand may be expressed as:

$$m\ddot{q} + c\dot{q} + kq = F \tag{1}$$

where m, c and k represent the mass, damping coefficient and spring stiffness, respectively. $\ddot{q}$, $\dot{q}$, q and F are related to parameters of acceleration, velocity, displacement and force,

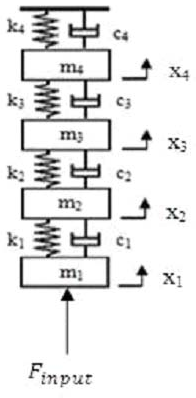

FIGURE 1. A 4-DOF palm model

respectively. In order to fully characterize the system, the state space model is used to derive the mathematical models of the 4-DOF system so that the internal system state is explicitly maintained over time, whereas with a transfer function, only the input-output relationship is maintained.

In matrix form, a continuous time state space model can be written as:

$$\dot{x}(t) = Ax(t) + Bu(t) \tag{2}$$

$$y(t) = Cx(t) + Du(t) \tag{3}$$

where
$\dot{x}$: state vector
y: output vector
u: input vector
A: state matrix
B: input matrix
C: output matrix
D: feedthrough matrix.

Thus, a 4-DOF model in continuous time has a state space model of the following form:

$$\ddot{x}_1 = -\frac{k_1}{m_1}x_1 - \frac{c_1}{m_1}\dot{x}_1 + \frac{k_1}{m_1}x_2 + \frac{c_1}{m_1}\dot{x}_2 + \frac{F(t)}{m_1} \tag{4}$$

$$\ddot{x}_2 = -\left(\frac{k_1+k_2}{m_2}\right)x_2 - \left(\frac{c_1+c_2}{m_2}\right)\dot{x}_2 + \frac{k_1}{m_2}x_1 + \frac{c_1}{m_2}\dot{x}_1 + \frac{k_2}{m_2}x_3 + \frac{c_2}{m_2}\dot{x}_3 \tag{5}$$

$$\ddot{x}_3 = -\left(\frac{k_2+k_3}{m_3}\right)x_3 - \left(\frac{c_2+c_3}{m_3}\right)\dot{x}_3 + \frac{k_2}{m_3}x_2 + \frac{c_2}{m_3}\dot{x}_2 + \frac{k_3}{m_3}x_4 + \frac{c_3}{m_3}\dot{x}_4 \tag{6}$$

$$\ddot{x}_4 = -\left(\frac{k_3+k_4}{m_4}\right)x_4 - \left(\frac{c_3+c_4}{m_4}\right)\dot{x}_4 + \frac{k_3}{m_4}x_3 + \frac{c_3}{m_4}\dot{x}_3 \tag{7}$$

The derivatives of x are given by:

$$\dot{x} = v \tag{8}$$

$$\ddot{x} = \dot{v} \tag{9}$$

$$y = x \tag{10}$$

After substituting the definitions of the states into the equations, the matrix form of A, B, C and D were obtained. Then, for a digital plant design, the continuous time plant is converted into a discrete equivalent state space by using Tustin operator-based continuous fraction expansion (CFE) scheme.

Table 1 shows the parameters used to emulate the motion of the hand palm model in the vertical plane. The parameters were suggested in an investigation in relation to ISO-10068* 4-DOF linear model [26]. It was chosen because the parameters are deemed appropriate and it is typically used in biodynamic behavior investigation.

In this simulation study, the parameters defining motion in the vertical direction are used to emulate the hand tremor.

TABLE 1. Parameters of skin anatomy at human hand [28]

Skin Layer	Mass, kg	Damper coefficient, Ns/m	Spring stiffness, N/m
Epidermis	0.0043	88.8	678
Dermis	0.105	1.5	185
Subcutaneous Tissue	0.566	0.1	23.9
Muscle	4.3	3.99	34.6

3. **Dynamic Modeling of Linear Voice Coil Actuators.** The Linear Voice Coil Actuator (LVCA) is employed as the main active element to counteract and suppress tremor. It has the capability to operate linearly, producing high stroke and block force that fully conform to the design requirements. LVCA consists of a cylindrical casing containing a permanent magnet which moves freely in a copper coil.

A magnetic field is produced when the current flows through the voice coil. The induced force produced is proportional to the current flowing through the coil. The direction of the force depends on the current direction. The current flow is reversed when the polarity of the applied voltage changes – moving the coil in an inverse direction. Thus, LVCA can perform in bidirectional (push and pull) mode with the desired supply frequency that is readily usable in vibration application. In addition, linear voice coil provides non-cogging, high speed, small hysteresis, excellent accuracy and repeatability.

The constitutive force equation of voice coil actuator follows the *Lorentz* force principle. The electromagnet field (EMF) generated is proportional to the rate of change of the magnetic flux. The movement of the charge q particle with a velocity $\vec{v}$ in an electromagnetic field will create a current (electric field $\vec{E}$ and magnetic field $\vec{B}$) [27]. Thus, the *Lorentz* force ($\vec{F}$) equation is given as follows:

$$\vec{F} = q\left(\vec{E} + \vec{v} \times \vec{B}\right) \tag{11}$$

Equation (11) shows the combination of electric and magnetic forces. In the macroscopic world, these forces are dominated by magnetic contribution, and the electrostatic contribution can be neglected. Suppose that if a current formed by a very large number of charged particles (the electrons) moving along the wire, the differential of force $\vec{\mathrm{d}}F$ of the field acting on an elementary length $\vec{\mathrm{d}}l$ of the wire is [27]:

$$\vec{\mathrm{d}}F = i\vec{\mathrm{d}}l \times \vec{B} \tag{12}$$

Thus, the total force is given by integrating

$$\vec{F} = i\int \vec{\mathrm{d}}l \times \vec{B} \tag{13}$$

Meanwhile, the *Lorentz* force of the magnetic field acting on the element $\mathrm{d}l = r\mathrm{d}\theta$ of one turn of the coil with a current i is describe as:

$$F = i\int r\mathrm{d}\theta.B \tag{14}$$

Thus, the relationship between the electromagnetic force F and the current of the coil i can be expressed as

$$F(t) = i(t)\,2\pi nrB \tag{15}$$

Hence, in *Laplace* transform, the above equation may be written as:

$$F(s) = K_F I(s) \tag{16}$$

where $K_F = 2\pi nrB$ is defined as the force sensitivity.

In this study, the LVCA used is the moving coil type, model NCC05-11-011-1X with force sensitivity, 5.2N/Amp [28]. The maximum voltage and current are 3V and 1A, respectively.

4. **Proposed Control Scheme.** The control scheme aims to suppress human hand tremor to zero tremor error. There are two types of feedback control methods proposed in the simulation study, namely, the Proportional-Integral-Derivative (PID) control and Active Force Control (AFC). The controllers are used to control the LVCA to cancel out the hand tremor.

4.1. **PID controller.** The PID controller is a three-term controller consisting of proportional, integral and derivative actions. PID control is the most common control algorithm and is frequently used to introduce newcomers to the basic concept of control system design. In this study, the PID control will be used to control the LVCA. Using the backward difference method, the discrete PID control law is described as:

$$G_c = G_P(k) + G_I(k) + G_D(k) \tag{17}$$

where $G_P(k)$, $G_I(k)$ and $G_D(k)$ are the transfer functions for the Proportional, Integral and Derivative component, respectively, and are defined as follows:

$$G_P(k) = K_P \tag{18}$$

$$G_I(k) = \frac{K_I T_s}{1 - z^{-1}} \tag{19}$$

$$G_D(k) = K_D \left[\frac{1 - z^{-1}}{T_s}\right] \tag{20}$$

Simplification of the above equations yields:

$$G_c(k) = K_P \left[e(k) - e(k-1)\right] + \frac{K_I T_s}{2}[e(k) + e(k-1)] + \frac{K_D}{T_s}\left[e(k) - 2e(k-1) + e(k-2)\right] \tag{21}$$

where K_P, K_I, K_D and T_s represent the proportional gain, integral gain, derivative gain and time constant, respectively.

4.2. **Active force control (AFC) theory.** The research of active force control (AFC) initiated by Johnson, and later Davison, is based on the principle of invariance and the classic *Newton's* second law of motion [29,30]. It has been demonstrated that it is possible to design a feedback controller that will ensure the system setpoint to remain unchanged even in the presence of disturbances or adverse operating and loading conditions provided that the actual disturbances can be modelled effectively. Hewit and Burdess proposed a more complete package of the system such that the nature of disturbances is oblivious to the system and that it is readily applied to multi-degree of freedom dynamic systems [31]. Thus, an effective method has been established to facilitate robust motion control of dynamic systems in the presence of the disturbances, parametric uncertainties and changes that are commonly prevalent in the real-world environment. Mailah et al. extended the usefulness of the method by introducing intelligent mechanisms to approximate the mass or inertia matrix of the dynamic system to trigger the compensation effect of the controller [22,32,33]. The AFC method is a technique that relies on the appropriate estimation of the inertial or mass parameters of the dynamic system and the measurements of the acceleration and force signals induced by the system. For theoretical simulation, perfect modelling of the sensors is assumed and that noises in the sensors are totally neglected. In AFC, it is shown that the system subjected to a number of disturbances remains stable and robust via the compensating action of the control strategy. A more detailed description of the mathematical treatment related to the derivation of important equations and stability criteria, can be found in [31,34]. For brevity, the underlying concept of AFC applied to a dynamic rotational system is presented with reference to Figure 2.

The notations used in Figure 2 are as follows:

θ_{d}: desired joint position

θ: actual joint position

K: constant gain

$G(s)$: dynamic system transfer function

$G_{\mathrm{a}}(s)$: Actuator transfer function

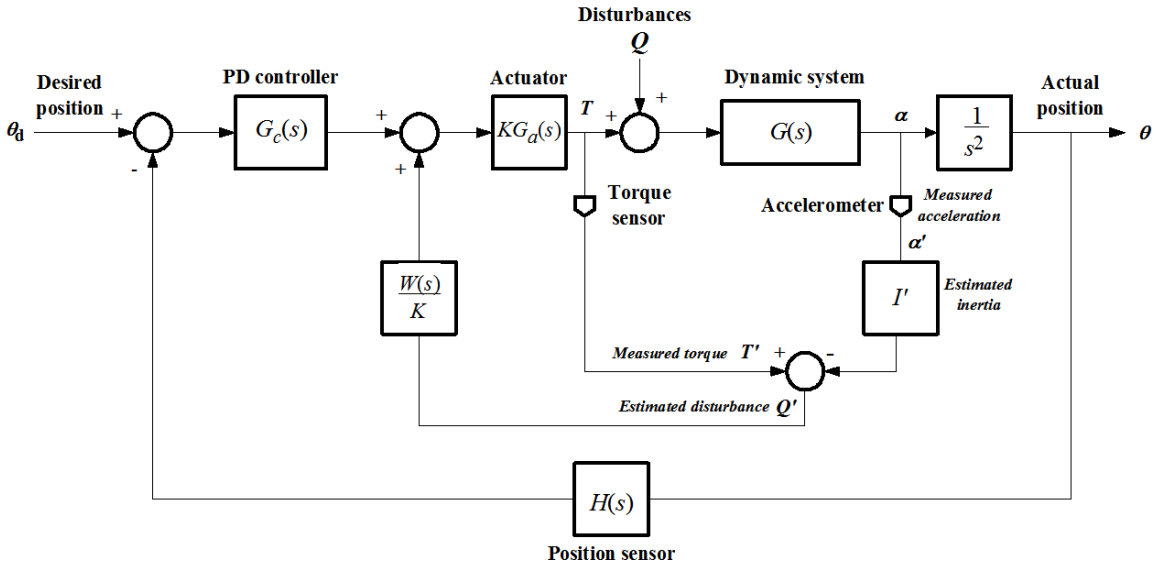

FIGURE 2. A schematic diagram of an AFC scheme

$G_c(s)$: Outer loop controller
$H(s)$: Sensor transfer function
$W(s)$: Weighting function
Q: Disturbances
T: applied torque
I: mass moment of inertia
α: angular acceleration.

The computed variable Q', known as the estimated disturbance, is obtained by considering the following expression:

$$Q' = T' - I'\alpha' \tag{22}$$

where the superscript $'$ denotes a measured, computed or estimated quantity. T' can be readily measured by means of a torque sensor and α' using an accelerometer. I' may be obtained by assuming a perfect model, crude approximation or intelligent methods [22]. Q' is then passed through a weighting function $W(s)$ to give the ultimate AFC signal command to be embedded with an outer control loop. This creates a two degree-of-freedom controller that can provide excellent overall system performance provided that the measurement and estimated parameters are appropriately acquired. The outermost control loop with the controller represented by $G_c(s)$ can be readily incorporated into the system such as those based on proportional-integral-derivative (PID), resolved motion acceleration controller (RMAC), computed torque and intelligent control techniques.

It is apparent that a suitable choice of $W(s)$ needs to be obtained that can enable the output θ to be made invariant with respect to the disturbances Q such that:

$$G_a(s)W(s) = 1 \tag{23}$$

In other words, if $W(s)$ is chosen as the inverse of $G_a(s)$ with $Q' = Q$, then perfect force control should be possible [31]. A set of outer control loop control is applied to the above open loop system, by first generating the global coordinate error vector, $e = (\theta_d - \theta)$ which would then be processed through a controller function, $G_c(s)$, typically a classic PD controller that maybe represented by:

$$u(s) = G_c(s)e(s) = (K_P + K_D s)e(s) \tag{24}$$

where
$u(s)$: control signal
$e(s)$: error signal
K_P: proportional gain
K_D: derivative gain.

It is common that the gains can be acquired using techniques such as *Ziegler-Nichols*, root locus or pole placement methods apart from heuristic means. The main computational burden in AFC is the multiplication of the estimated inertial parameter with the angular acceleration of the dynamic component before being fed into the AFC feedforward loop.

5. **PSO Versus DE Optimization Techniques.** PSO and DE optimization techniques are used to estimate the K_P, K_I and K_D values in PID control and the estimated mass, M' in the AFC scheme. Based on the information of the track error (denoted by e), the optimization work is started by optimizing the PID parameters first without the effect of AFC control. After that, using the optimal PID parameters, the M' gain is estimated and fed into the AFC feed-forward loop. The optimization processes are run separately to investigate and compare the effect between the PID control and hybrid control (PID + AFC control) on the motion of 4-DOF hand model. Figure 3 illustrates the proposed optimization technique in optimizing the controller gains and estimated mass.

The optimal values for PID and M' parameters are based on the performance of the fitness function. In this paper, the integral of absolute error (IAE) is used as the performance index. IAE sums up the areas above and below the set point, thereby penalizes all errors equally regardless of the direction. A lower score of IAE represents a higher fitness of the individual. For stopping criterion, the maximum number of generations is used when the cycle of evolution is repeated until the 70^{th} loop.

The schematic in Figure 3 is the proposed 2-DOF controller (PID outer loop and AFC inner loop) that offers excellent overall system performance provided that the measured and estimated parameters had been appropriately acquired. For theoretical simulation, it is assumed that the position sensor gives a perfect modeling ($H_s(s) = 1$) and that the noises in the sensors are negligible. The details of the GA and PSO operation techniques are presented in the following sections.

5.1. **Particle swarm optimization.** Particle Swarm Optimization (PSO) is a population based stochastic optimization technique, which imitates the concept of social behavior

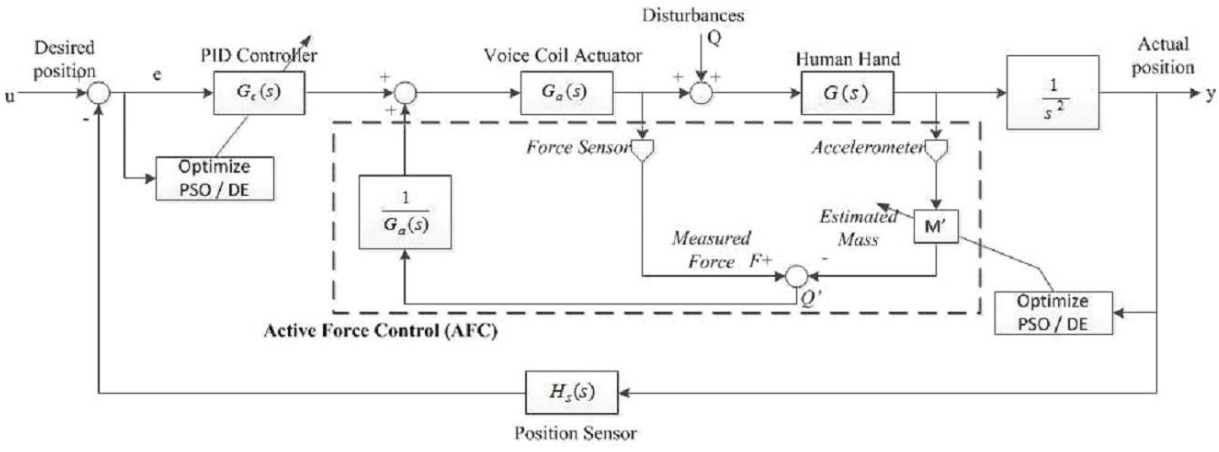

FIGURE 3. A schematic diagram of the proposed control design

of bird flocks searching for corn and fish schooling [14]. PSO is initialized with a random population of particles, their positions and velocities in which all of them have the same number of size. Then, each particle is coupled with a velocity vector and swarms through the D-dimensional search space of the problem. The particles will memorize the best ever position that has been reached in the search space. This position is defined as *pbest*. The trajectory of the particle is dynamically adjusted based on its performance and the performance of their neighboring particles.

Thus, the particles keep on improving simultaneously with subsequent generations in search for better exploration to find the global optimum. The key success of the PSO algorithm is the clever exchange of information about the global and local best values. The "global" version of the particle swarm optimizer keeps track among the best values of *pbest*, called *gbest* [35]. In order to estimate the best update for the position in the next iteration, each particle parameter is manipulated according to the following expressions:

- Velocity of individual particles

$$v_{k+1}^i = \omega v_k^i + c_1 r_1 (p_k^i - x_k^i) + c_2 r_2 \left(p_k^g - x_k^i\right) \tag{25}$$

- Position of individual particles

$$x_{k+1}^i = x_k^i + v_{k+1}^i \tag{26}$$

where x_k^i is the particle position, v_{k+1}^i is the particle velocity, ω is the inertia weight, p_k^i is the best individual particle position, p_k^g is the best swarm position c_1, c_2 are the cognitive and social parameters respectively, and r_1, r_2 are random numbers between 0 and 1. The flying direction of each particle is influenced by three types of information known as present motion, individual knowledge and social knowledge. Then, the next position of the particle will be updated by combining all the information with the current particle position. The computational flow chart of the PSO algorithm is shown in Figure 4.

5.2. **Differential evolution.** Differential Evolution (DE) is one of meta-heuristic methods and is a powerful tool to find global optimal solution. The main idea of differential evolution (DE) algorithm is to avoid greedy search in which the fast convergence possible trapped by local minima. Thus, by using parallel direct search technique and running several vectors simultaneously, the problem can be countered.

In this algorithm, the first variant of DE scheme, type DE/rand/1, is implemented as a mutation operator [17]. The notation 'rand' relates to the technique for searching the base vector, while '1' indicates the number of difference vectors used to perturb the base vector. The new parameter vector is generated by manipulating three random choosen parameters $r1$, $r2$, $r3$ from a population $\{1, \ldots, m\}$ and different from the index i; by means of the following equation:

$$v_i = x_{r1} + F\left(x_{r2} - x_{r3}\right) \tag{27}$$

where the differentiation constant F refers to scaling factor $[0, 1+]$ of different vectors which control the exploitation and exploration of the search space. As the number of generations increases, the search step length becomes smaller and finally makes the DE to converge.

The crossover operator function was performed after mutation to increase the diversity of the population. Here, the binomial crossover variant is used and the scheme is described as follows:

$$u_{i,j} = \begin{cases} v_{i,j} & \text{if } (rand_{ij}[0,\,1) \leq Cr) \text{ or } (Rnd = i) \\ x_{i,j} & \text{otherwise} \end{cases} \tag{28}$$

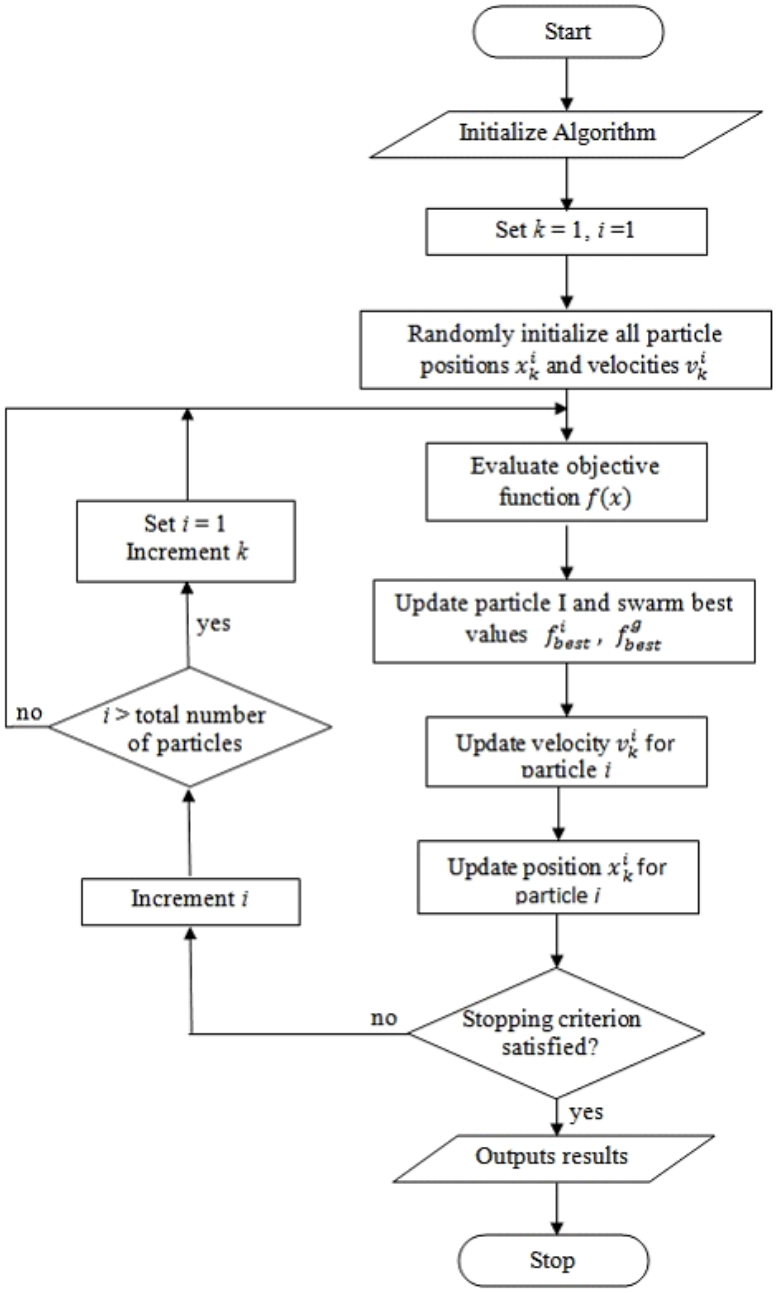

FIGURE 4. Flowchart of the PSO algorithm

where the Cr is the crossover rate value, $Cr \in [0, 1]$. $Cr = 0$ refers to absence of parent effect while $Cr = 1$ means inherit current population. The parameter Rnd is randomly chosen from problem dimension $\{1, 2, \ldots, D\}$ range. This is to confirm that at least one of the parameters obtains from mutant vector [17].

In the selection process, the fitness function of the new and current individuals will be compared. The selection scheme may be described as:

$$x_{i,G+1} = \begin{cases} u_{i,G} & \text{if } f(u_{i,G}) \leq f(x_{i,G}) \\ x_{i,G} & \text{if } f(u_{i,G}) > f(x_{i,G}) \end{cases} \tag{29}$$

If the new trial individual, $u_{i,G}$, is less or similar to the fitness function value of the corresponding vector, $x_{i,G}$, then it replaces the corresponding vector in the next generation, $x_{i,G+1}$; otherwise, the vector retains its place in the population. As shown in Figure

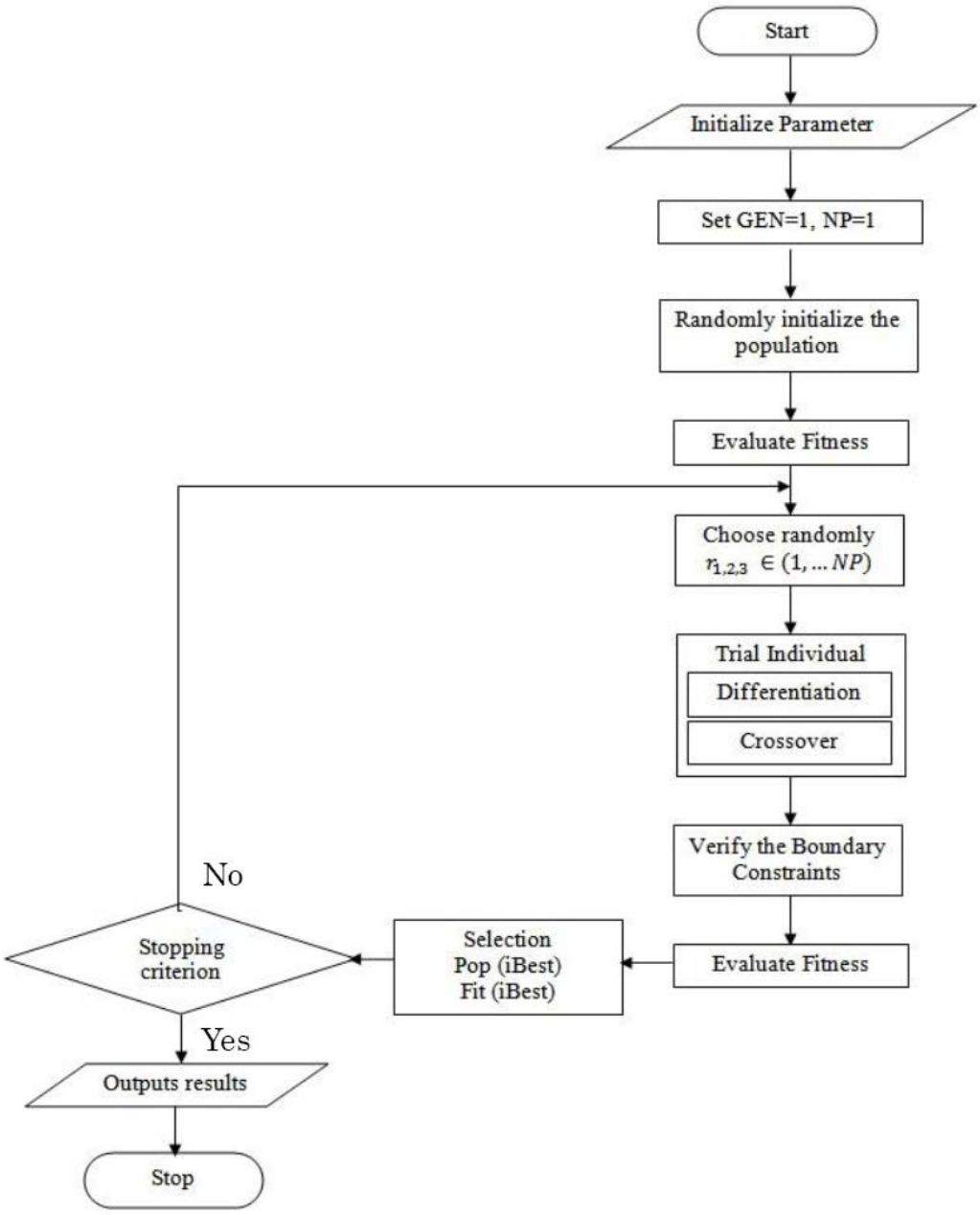

FIGURE 5. Flowchart of the DE algorithm

5, only the best individual will remain as the best population until the last generation or termination criterion is satisfied. Thus, the fitness function keeps on improving or remains constant with the increase generation.

6. **Results and Discussion.** The behavior of the 4-DOF biodynamic model of hand tremor will be demonstrated here considering the PID and PID + AFC controller. In this simulation study, the PID parameters will be first optimized using the PSO and DE algorithms. Next, the estimated mass, M' parameter in the AFC controller is optimized using the same proposed optimization technique. While applying PSO and DE, a number of parameters are required to be specified as shown in Table 2. The following selected parameters are those that give the best computational results in suppressing the hand tremor.

TABLE 2. Parameters used in a PSO and DE

Parameters	Value
Min. $[K_P, K_I, K_D, M']$ for PSO	$[0, 0, 0, 0]$
Min. $[K_P, K_I, K_D, M']$ for DE	$[0, 0, 0, 0]$
Max. $[K_P, K_I, K_D, M']$ for PSO	$[200, 200, 200, 30]$
Max. $[K_P, K_I, K_D, M']$ for DE	$[200, 200, 200, 30]$
Number of generation for PSO	70
Number of generation for DE	70
Number of Swarm	50
Population size of DE	50
CR	0.9
F	0.4
c_1	2
c_2	2
w	0.8

TABLE 3. Parameters computed in PSO and DE

Parameters	PSO	DE
K_P	189.25	197.66
K_I	41.73	172.98
K_D	198.82	199.96
M'	0.4823	0.1501
IAE level (PID)	0.1691	0.1681
IAE level (PID + AFC)	0.1270	0.1207

Figure 6(a) illustrates the convergence of the objective function with the number of generations for PSO and DE within 70 generations. Figure 6(b) depicts the effect of AFC on the convergence rate. Obviously, with the presence of AFC scheme, the convergence rate of IAE levels for both PSO and DE are lower, thereby, implying higher performance of the optimization parameters. Based on the performance calculation with respect to the fitness value, AFC improves the performance of the PID controller by approximately 24.90% for PSO and 28.20% for DE.

The DE shows fast convergence and better IAE performance compared with PSO. For the complex plant model (4-DOF hand tremor) using the PID controller, the DE effectively starts converging to the global optimum at the 11^{th} generation while the PSO seems to be trapped in local minima at the 20^{th} generation (see Figure 6(a)). For the hybrid controller shown in Figure 6(b), the DE is able to find the optimal solution in which the convergence rate of IAE level for DE is much smaller than PSO. The AFC scheme offers rapid convergence for both optimization methods due to the lesser computational process and the fact that only one parameter is to be optimized. In order to make sensible comparison, Table 3 indicates the optima value of the proposed controller parameters obtained by PSO and DE algorithms.

6.1. **Displacement response.** Using an active control method to suppress hand tremor, the effectiveness of the controllers and the optimization methods employed for the 4-DOF biodynamic model of the human hand tremor shall be compared. Figures 7 and 8 exhibit the comparison of the performance of the controllers PID and PID + AFC for both PSO and DE methods. Referring to Figures 7(a) and 8(a), the simulated hand tremor was

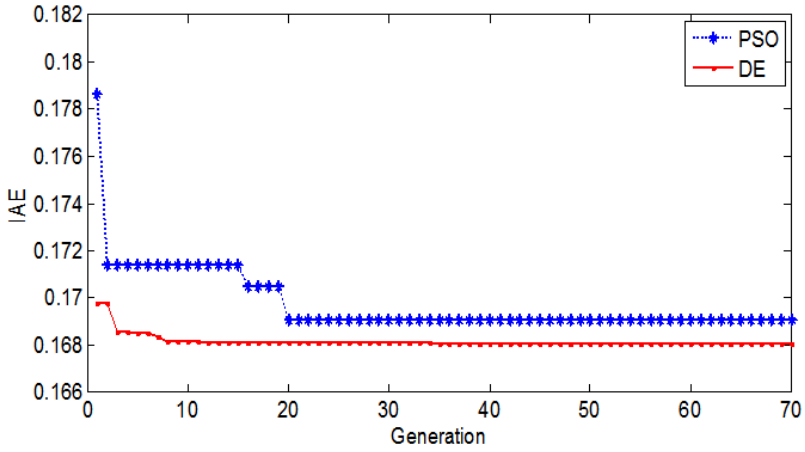

(a) PID control

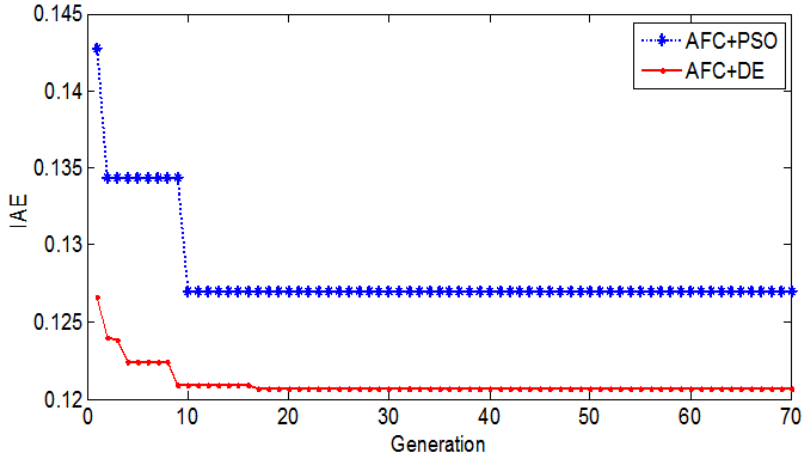

(b) PID + AFC control

FIGURE 6. Comparison of convergence of objective function

created between −5 mm and 5 mm and plot was labeled as 'Hand Tremor'. It looks like a rhythmic sinusoidal behaviour that emulates the actual human postural tremor behavior [36].

In time domain as shown in Figures 7(a) and 8(a), the oscillations of the tremor suppression for the PID and PID + AFC controllers do not show visible differences between the PSO and DE techniques. This is probably due to the fact that the optimal values obtained from both optimization methods are very close as shown in Table 4. During the 10s simulation period, by using the PID controller, the displacement response of the human hand tremor oscillates between $\pm 4 \times 10^{-4}$m. By adding the AFC scheme, the hand tremor error is reduced to $\pm 2 \times 10^{-4}$ m for both PSO and DE methods.

Figures 7(b) and 8(b) show the results of the hand tremor in frequency domain using the PSO and DE techniques, respectively. The coherence frequency of the 4-DOF biodynamic hand tremor occurred at 8.984 Hz with the maximum peak at 2.412 m^2/Hz. The findings are in good agreement with the actual human hand tremor which mostly occurs within the range, 4-12 Hz [33,34]. By using the PSO technique, the hand tremor peak is reduced by 89.83% (for PID) and 93.81% (for PID + AFC). Meanwhile, by using the DE technique, the hand tremor peak is reduced by 89.89% (for PID) and 93.85% (for PID + AFC). The findings prove that the hybrid controller optimized by PSO and DE was able to suppress

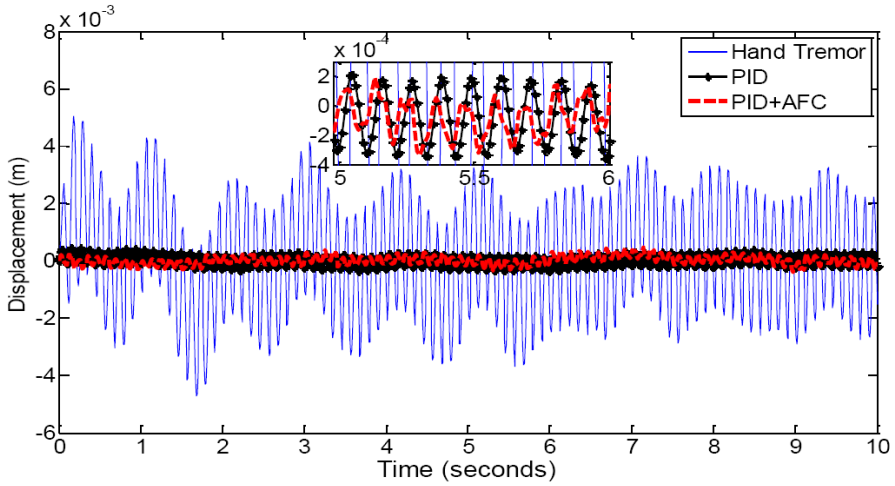

(a) Time domain

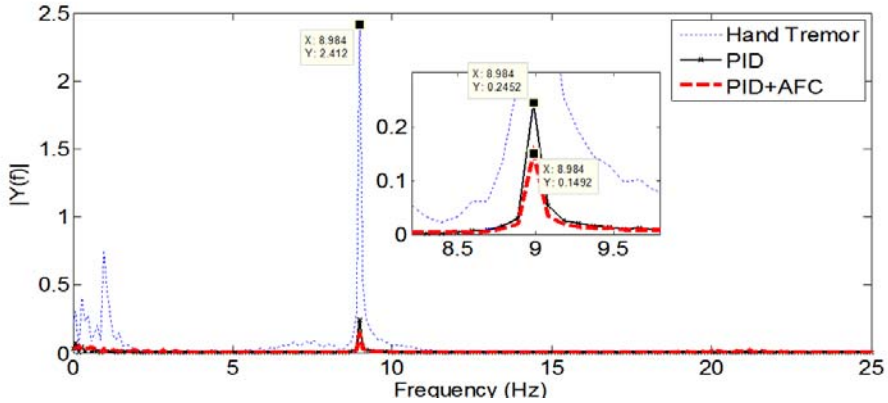

(b) Frequency domain

FIGURE 7. Displacement behavior of the hand tremor using PSO

TABLE 4. Comparison of frequency peaks obtained by PSO and DE for displacement behavior

Parameters	PSO	DE
Human Hand	2.412 m^2/Hz	2.412 m^2/Hz
PID	0.2452 m^2/Hz	0.2438 m^2/Hz
PID + AFC	0.1492 m^2/Hz	0.1484 m^2/Hz

the tremor and led the human hand oscillation close to zero datum (no tremor). Table 4 summarizes the comparison of the frequency peaks between the PSO and DE methods.

6.2. **Acceleration response.** The corresponding results for the acceleration behavior of the hand tremor are shown in Figures 9 and 10. Figures 9(a) and 10(a) exhibit results in time domain for PSO and DE respectively. Note that the tremor peak-to-peak acceleration amplitude is within the range of $\pm 8 m/s^2$. However, unlike the displacement results, the oscillation of acceleration signal when using AFC + PID controller is greater than the PID control. This is due to the presence of noise in the acceleration signal, which is the important parameter to be multiplied with the estimated mass, M' (using the meta-heuristic method) before being fed into the AFC feed-forward loop. In practice, the

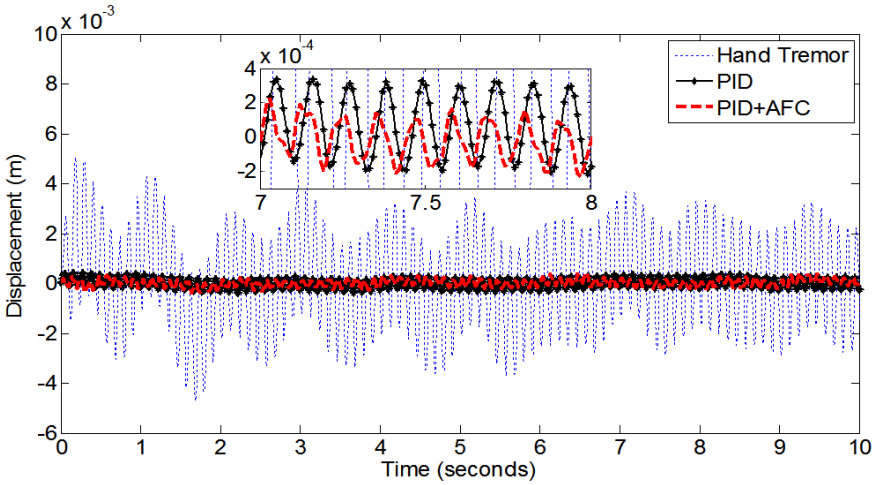

(a) Time domain

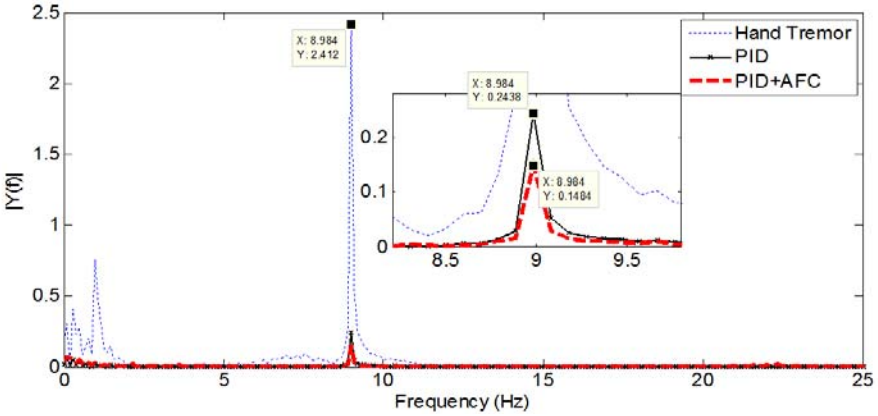

(b) Frequency domain

FIGURE 8. Displacement behavior of the hand tremor using DE

accelerometer is always exposed to some form of noises such as the wiring noise or those from other electrical devices.

After conversion to the Fast Fourier Transform (FFT) analysis, the frequency peak of the hand tremor using the AFC based scheme is still much lower than the PID counterpart. This can be confirmed by observing the frequency plots in Figures 9(b) and 10(b) which are related to the optimization using the PSO and DE methods, respectively. The coherence frequency of the simulated hand tremor synchronised with the displacement response is at 8.984 Hz and the maximum peak is at 7497 $(\mathrm{m/s^2})^2/\mathrm{Hz}$. By using the PSO method, the frequency peak for the PID control is reduced by 89.86%. However, for the PID + AFC control the peak is further decreased to 93.80%. Meanwhile, by using the DE technique (see Figure 10), the vibration level of the PID control is reduced by 89.91% and for the hybrid control, it is 93.86%. The comparison of the frequency peaks obtained by the PSO and DE techniques are shown in Table 5. The findings actually reveal that the PID + AFC control scheme also provides better improvements for tremor attenuation with reference to the acceleration behaviour.

Overall, it can be deduced that when the AFC-based controller is employed, there is a significant reduction in the hand tremor error. The acceleration amplitude signal result in time domain is not favorable, but in spectral measurement the peak still shows lower magnitude (compared with PID) for the same frequency of interest at 8.984 Hz. The DE

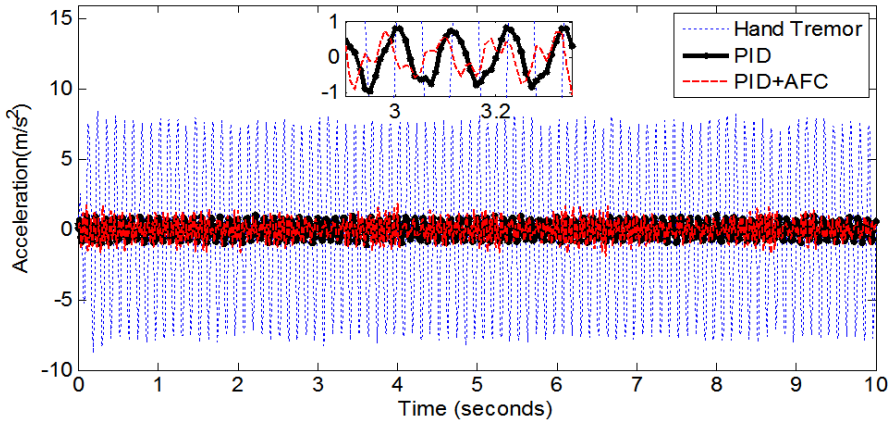

(a) Time domain

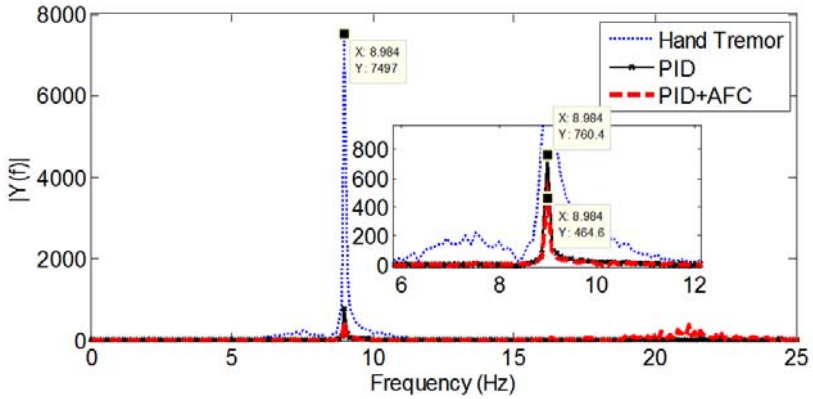

(b) Frequency domain

FIGURE 9. Acceleration behavior of hand tremor using PSO

TABLE 5. Comparison of the frequency peaks obtained by PSO and DE for the acceleration behavior

Parameters	PSO	DE
Human Hand	7497 $(m/s^2)^2/Hz$	7497 $(m/s^2)^2/Hz$
PID	760.4 $(m/s^2)^2/Hz$	756.1 $(m/s^2)^2/Hz$
PID + AFC	464.4 $(m/s^2)^2/Hz$	460.6 $(m/s^2)^2/Hz$

shows good performance and is more robust (based on the IAE performance to achieve global optimal value) compared to the PSO scheme. Moreover, the DE algorithm is easy to implement, less computationally complex, and has fewer parameters to fine-tune. Theoretically, the findings prove that the PID and PID + AFC controllers work well with the linear voice coil actuator and give good response in suppressing the human hand tremor. The feedback from the tremor error gives response to the controller to drive the bidirectional actuator with certain speed. Hence, the actuator is capable of producing counter signals to cancel out the vibration effect from the hand tremor.

7. **Conclusions.** This paper evaluates the performance evaluation of two types of closed loop feedback control, namely, PID control and PID+AFC control, in an effort to suppress human hand tremor. Novel PSO and DE based approaches have been successfully

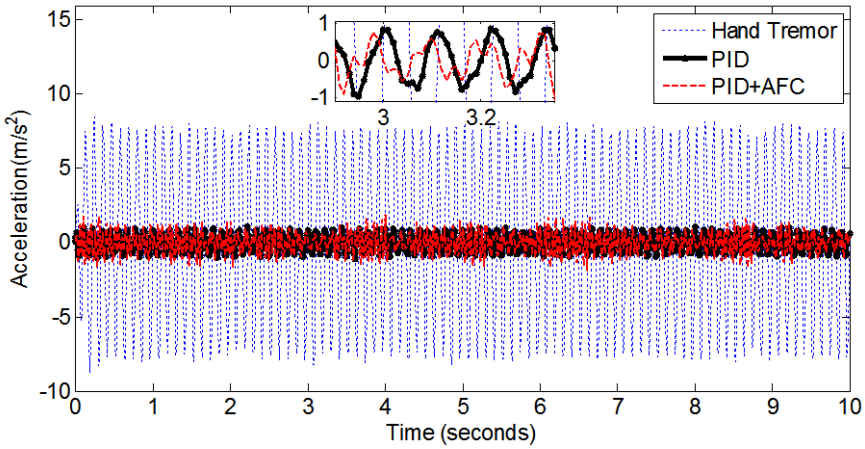

(a) Time domain

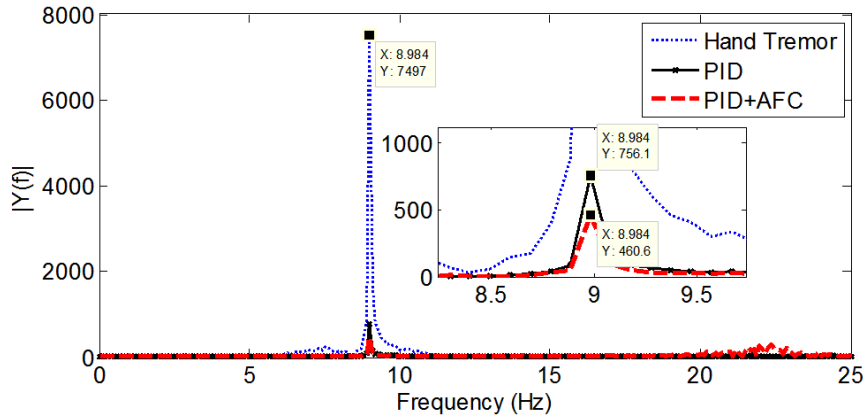

(b) Frequency domain

FIGURE 10. Acceleration behavior of hand tremor using DE

implemented to optimally design the PID and AFC controllers for the linear voice coil actuation. From the findings, the hybrid PID + AFC controller shows excellent performance in reducing the tremor error significantly. Based on the performance fitness evaluation, the AFC based scheme is able to enhance the PID performance using both PSO and DE techniques. The DE is shown to have better fitness function and faster convergence compared with the PSO counterpart. The preliminary outcomes of the study may assist in the design and development of anti tremor equipment utilizing linear voice coil actuator. Real time implementation using AFC-based scheme for the purpose of tremor suppression is on-going and serves as a useful validation tool based on the proposed strategies considered in the study.

Acknowledgment. The authors would like to thank the Malaysian Ministry of High Education (MOHE) and Universiti Teknologi Malaysia (UTM) for their continuous support in the research work. This work was financially supported in part by the Malaysia FRGS Fund under Grant Vote No: 78510.

REFERENCES

[1] B. Pellegrini, L. Faes, G. Nollo and F. Schena, Quantifying the contribution of arm postural tremor to the outcome of goal-directed pointing task by displacement measures, *Journal of Neuroscience Methods*, vol.139, no.2, pp.185-193, 2004.

[2] J. Carr, Tremor in Parkinson's disease, *Parkinsonism & Related Disorder*, vol.8, no.4, pp.223-234, 2002.
[3] A. Carlsson, P. Greengard and E. Kandel, Signal transduction in the nervous system, *The Nobel Prize in Physiology or Medicine*, Karolinska Institute, 2000.
[4] B. Ford, *Deep Brain Stimulation for Parkinson's Disease*, Parkinson Disease Foundation, 3rd Edition.
[5] W. Poewe, A. Antonini, J. C. M. Zijlmans, P. R. Bukhard and F. Vingerhoets, Levadopa in the treatment of Parkinson's disease: An old drug still going strong, *Clinical Interventions in Aging*, vol.5, pp.229-238, 2010.
[6] C. N. Kong, Brain surgery in Parkinson's disease (PD) – The Malaysian experience, *Educational Resources, Pantai Holding Berhad*, http://www.pantai.com.my/docs-writeup/brain-surgery-in-parkinsons-disease-pd-the-malaysian-experience/#.Ttxs1LK4qdA, 2007.
[7] E. Rocon, J. M. Belda-Lois, A. F. Ruiz, M. Manto, J. C. Moreno and J. L. Pons, Design and validation of rehabilition robotic exoskeleton for tremor assessment and suppression, *IEEE Trans. on Neural Systems and Rehabilition Engineering*, vol.15, no.3, pp.367-378, 2007.
[8] D. Zhang, P. Poignet, F. Widjaja and W. T. Ang, Neural oscillator based control pathological tremor suppression via functional electrical stimulation, *Control Engineering Practice*, vol.19, pp.74-88, 2011.
[9] D. Case, B. Taheri and E. Richer, Design and characterization of a small-scale magnetorheological damper for tremor suppression, *IEEE/ASME Trans. on Mechatronics*, pp.1-8, 2011.
[10] J. Kennedy and R. C. Eberhart, Particle swarm optimization, *Proc. of 1995 IEEE International Conference on Neural Networks*, Perth, Australia, vol.4, pp.1942-1948, 1995.
[11] G. D. Li, S. Masuda, D. Yamaguchi and M. Nagai, The optimal GNN_PID control system using particle swarm optimization algorithm, *International Journal of Innovative Computing, Information and Control*, vol.5, no.10(B), pp.3457-3469, 2009.
[12] Y. Wakasa, K. Tanaka, T. Akashi and Y. Nishimura, PSO-based simultaneous tuning method for PID controllers and dead-zone compensators and its application to ultrasonic motors, *International Journal of Innovative Computing, Information and Control*, vol.6, no.10, pp.4593-4604, 2010.
[13] A. Alfi, Particle swarm optimization algorithm with dynamic inertia weight for online parameter identification applied to lorenz chaotic system, *International Journal of Innovative Computing, Information and Control*, vol.8, no.2, pp.1191-1203, 2012.
[14] R. Storn and K. Price, Differential evolution: A simple and efficient adaptive scheme for global optimization over continuous spaces, *Journal of Global Optimization*, vol.11, no.4, pp.341-359, 1997.
[15] A. Biswas, S. Das, A. Abraham and S. Dasgupta, Design of fractional-order PID controllers with an improved differential evolution, *Engineering Applications of Artificial Intelligence*, vol.22, no.2, pp.343-350, 2009.
[16] V. Vegh, G. K. Pierens and Q. M. Tieng, A variant of differential evolution for discrete optimization problems requiring mutually distinct variables, *International Journal of Innovative Computing, Information and Control*, vol.7, no.2, pp.897-914, 2011.
[17] V. Feoktistov, Differential evolution – In search of solutions, *Optimization and Its Applications*, vol.5, 2006.
[18] M. Mailah, J. R. Hewit and S. Meeran, Active force control applied to a rigid robot arm, *Journal Mekanikal*, vol.2, no.2, pp.52-68, 1996.
[19] E. Pitowarno, M. Mailah and H. Jamaluddin, Knowledge-based trajectory error pattern method applied to an active force control scheme, *International Journal of Engineering and Technology*, vol.2, no.1, pp.1-15, 2002.
[20] A. Noshadi, M. Mailah and A. Zolfagharian, Intelligent active force control of a 3-RRR parallel manipulator incorporating fuzzy resolved acceleration control, *Applied Mathematical Modelling*, vol.36, no.6, pp.2370-2383, 2012.
[21] M. Mailah, M. Y. Wong and H. Jamaluddin, Intelligent active force control a robot arm using genetic algorithm, *Journal Mekanikal*, vol.13, pp.50-63, 2002.
[22] M. Mailah, *Intelligent Active Force Control of a Rigid Robot Arm Using Neural Network and Iterative Learning Algorithms*, Ph.D. Thesis, University of Dundee, UK, 1998.
[23] G. Priyandoko, M. Mailah and H. Jamaluddin, Vehicle active suspension system using skyhook adaptive neuro active force control, *Mechanical Systems and Signal Processing*, vol.23, no.3, pp.855-868, 2009.
[24] H. Jahanabadi, M. Mailah, M. Z. Md. Zain and H. H. Mun, Active force with fuzzy logic control of a two-link arm driven by pneumatic artificial muscles, *Journal of Bionics Engineering*, vol.8, no.4, pp.474-484, 2011.

[25] A. As'arry, M. Z. Md. Zain, M. Mailah, M. Hussein and Z. M. Yusop, Active tremor control in 4-DOFs biodynamic hand model, *International Journal of Mathematical Models and Method in Applied Sciences*, vol.5, no.6, pp.1068-1076, 2011.

[26] S. Rakheja, J. Z. Wu, R. G. Dong, A. W. Schopper and P. É. Boileau, A comparison of biodynamic models of the human hand-arm system for applications to hand-held power tools, *Journal of Sound and Vibration*, vol.249, no.1, pp.55-82, 2002.

[27] A. Preumont, Mechatronics, *Solid Mechanics and Its Applications*, Springer, 2006.

[28] *Linear Voice Coil NCC05-11-011-1X Data Sheet*, http://www.h2wtech.com/pdf/30-0126%20Rev%20B%20NCC05-11-011-1X.pdf, 2012.

[29] C. D. Johnson, Accommodation of external disturbances on linear regulator and servomechanism problems, *IEEE Trans. on Automat. Control*, vol.16, no.6, pp.635-644, 1971.

[30] E. J. Davison, Multivariable tuning regulators: The feedforward and robust control of a general servomechanism problem, *IEEE Trans. on Automat. Control*, vol.21, pp.35-47, 1976.

[31] J. R. Hewit and J. S. Burdess, Fast dynamic decoupled control for robotics using active force control, *Trans. on Mechanism and Machine Theory*, vol.16, no.5, pp.535-542, 1981.

[32] M. Mailah and M. Y. Ong, Intelligent adaptive active force control of a robot arm with embedded iterative learning algorithms, *Journal Teknologi*, no.35, pp.85-98, 2001.

[33] M. Mailah, E. Pitowarno and H. Jamaluddin, Robust motion control for mobile manipulator using resolved acceleration and proportional-integral active force control, *International Journal of Advanced Robotic Systems*, vol.2, no.2, pp.125-134, 2005.

[34] J. S. Burdess and J. R. Hewit, An active method for the control of mechanical systems in the presence of unmeasurable forcing, *Trans. on Mechanism and Machine Theory*, vol.21, no.3, pp.393-400, 1986.

[35] R. Eberhart and J. Kennedy, A new optimizer using particle swarm theory, *Proc. of the 6th International Symposium on Micro Machine and Human Science*, Nagoya, Japan, pp.39-44, 1995.

[36] D. E. Vaillancourta, A. B. Slifkina and K. M. Newella, Regularity of force tremor in Parkinson's disease, *Clinical Neurophysiology*, vol.112, no.9, pp.1594-1603, 2001.